Early Identification of Retinal Neuropathy in Subclinical Diabetic Eyes by Reduced Birefringence of the Peripapillary Retinal Nerve Fiber Layer

Andreas Pollreisz,[1] Sylvia Desissaire,[2] Aleksandra Sedova,[1] Dorottya Hajdu,[1] Felix Datlinger,[1] Florian Schwarzhans,[3] Stefan Steiner,[1] Irene Steiner,[3] Clemens Vass,[1] Christoph K. Hitzenberger,[2] Michael Pircher,[2] and Ursula Schmidt-Erfurth[1]

[1]Department of Ophthalmology and Optometry, Medical University Vienna, Vienna, Austria
[2]Center for Medical Physics and Biomedical Engineering, Medical University of Vienna, Vienna, Austria
[3]Center for Medical Statistics, Informatics and Intelligent Systems, Section for Medical Statistics, Medical University Vienna, Vienna, Austria

Correspondence: Andreas Pollreisz, Department of Ophthalmology and Optometry, Medical University Vienna, Waehringer Guertel 18-20, 1090 Vienna, Austria; andreas.pollreisz@meduniwien.ac.at.

Received: August 13, 2020
Accepted: March 19, 2021
Published: April 19, 2021

Citation: Pollreisz A, Desissaire S, Sedova A, et al. Early identification of retinal neuropathy in subclinical diabetic eyes by reduced birefringence of the peripapillary retinal nerve fiber layer. *Invest Ophthalmol Vis Sci.* 2021;62(4):24. https://doi.org/10.1167/iovs.62.4.24

Purpose. To study birefringence of the peripapillary retinal nerve fiber layer (RNFL) of diabetic eyes with no clinical signs of diabetic retinopathy (DR) or mild to moderate DR stages using spectral-domain polarization-sensitive (PS) optical coherence tomography (OCT).

Methods. In this observational pilot study, circular PS-OCT scans centered on the optic nerve head were recorded in prospectively recruited diabetic and age-matched healthy eyes. From averaged circumpapillary intensity and retardation tomograms plots of RNFL birefringence were obtained by a linear fit of retardation versus depth within the RNFL tissue for each A-scan position and mean birefringence values for RNFL calculated. Spectral-domain OCT imaging (Heidelberg Engineering) was performed to assess peripapillary RNFL thickness and macular ganglion cell complex (GCC).

Results. Out of 70 eyes of 43 diabetic patients (mean ± SD age: 50.86 ± 15.71) 36 showed no signs of DR, 17 mild and 17 moderate nonproliferative DR with no diabetic macular edema. Thirty-four eyes of 34 healthy subjects (53.21 ± 13.88 years) served as controls. Compared with healthy controls (0.143° ± 0.014°/µm) mean total birefringence of peripapillary RNFL was significantly reduced in subclinical diabetic eyes (0.131° ± 0.014°/µm; $P = 0.0033$), as well as in mild to moderate DR stages (0.125° ± 0.018°/µm , $P < 0.0001$) with borderline statistically significant differences between diabetic patients ($P = 0.0049$). Mean birefringence values were significantly lower in inferior compared with superior RNFL sectors ($P < 0.0001$) of diabetic eyes with no such difference detected in the healthy control group.

Conclusions. We identified evidence of early neuroretinal alteration in diabetic eyes through reduced peripapillary RNFL birefringence assessed by PS-OCT occurring before appearance of clinical microvascular lesions or GCC alterations.

Keywords: diabetic retinopathy, PS-OCT, retinal nerve fiber layer, birefringence

Diabetic retinopathy (DR) is the leading cause of irreversible but preventable blindness in working-age adults worldwide caused by microvascular and neurodegenerative damages to the retina.[1,2] Retinal diabetic neuropathy (RDN) occurs early during the pathogenesis of DR and may even be present in the absence of clinically detectable microvasculopathy.[2] Characteristic alterations in retinal neural structures include loss of ganglion cells, neural apoptosis, and reactive gliosis combined with thinning of the inner retina. Functional changes observed in these patients are dysfunctional dark adaptation,[3] deficits in contrast sensitivity,[4] altered perimetry tests,[5,6] as well as abnormal pattern[7] and multifocal electroretinograms.[5] The second innermost layer of the retina consists of the retinal nerve fiber layer (RNFL), which is composed of unmyelinated axons of the ganglion cells. Their thickest dimensions are located around the optic nerve and decrease toward the peripheral retina. As ocular optical components allow unobstructed observations of neural tissues in the living human eye, RNFL can be imaged with optical coherence tomography (OCT) technology.[8] In a number of ocular and systemic diseases, such as glaucoma,[9] multiple sclerosis,[10] Parkinson,[11] and Alzheimer diseases,[12] thinning of peripapillary RNFL has been observed by OCT.

Polarization-sensitive (PS)-OCT[13–18] is a functional extension of conventional intensity-based OCT combining depth-resolved retinal images with the polarization sensitivity of scanning laser polarimetry (SLP),[19] allowing the

quantification of RNFL birefringence.[16,20–23] Different retinal layers show specific polarizing properties and can be differentiated into polarization maintaining structures, including the photoreceptor layer, depolarizing layers, such as the retinal pigment epithelium,[24,25] and birefringent structures encompassing the retinal nerve fiber and Henle fiber layer.[24,26–29] The main benefit of PS-OCT imaging is its potential to simultaneously and independently measure retardation and thickness of RNFL.

To the best of our knowledge, no comprehensive study comparing RNFL birefringence between diabetic and healthy subjects has been performed. A recently published pilot study by our group analyzed the repeatability of RNFL birefringence calculation and only gave a limited comparison between the results in a small subset of healthy subjects (n = 7) and diabetic patients with mild or moderate DR (n = 7).[30] The present study focuses on a more detailed quantitative and statistically relevant comparison by PS-OCT aiming to quantify peripapillary RNFL birefringence values in eyes with different DR stages ranging from subclinical to moderate DR, differentiating between superior and inferior peripapillary segments and including clinical parameters such as HbA1c levels or diabetes duration.

Subjects and Methods

The research adhered to the tenets of the Declaration of Helsinki and the Good Clinical Practice guidelines. Institutional review board approval was obtained at the Medical University Vienna, and all participants provided written informed consent before study inclusion.

Patients and healthy control subjects were recruited at the Department of Ophthalmology and Optometry at the Medical University Vienna.

We included adult type 1 or 2 diabetic patients with mild or moderate nonproliferative DR and no clinically detectable DR as assessed on detailed funduscopy including far peripheral retinal regions at the slit lamp and additionally analyzing widefield images performed with Optomap (California, Optos). The healthy nondiabetic control group consisted of age-matched subjects with one randomly selected eye included without any ocular disease, except cataract. In both the diabetic and healthy control group, a Spectralis peripapillary RNFL scan was performed and only subjects within normal limits (see description later) were included in the analysis. Exclusion criteria in the diabetic group were present or past diabetic macular edema (DME), proliferative DR, intravitreal injection of anti-VEGF or corticosteroids, retinal photocoagulation, previous ocular surgeries except cataract surgery (at least 6 months prior to study inclusion), any other ocular disease. Exclusion criteria for the healthy control group were any past or present ocular diseases except cataract or any ocular surgeries except cataract extraction at least 6 months prior to study inclusion. Other exclusion criteria for both groups were refractive errors over +2 or under −3 diopters. The stage of DR in the diabetic group was classified based on the Early Treatment Diabetic Retinopathy Study (ETDRS) classification. The grading of the severity of DR was done by two trained graders on Optomap fundus images with superimposed seven-fields (not on fundus photography).[31] Both eyes of diabetic patients were included if eligible. In the healthy subject group only one eye was included. After ETDRS best-corrected visual acuity (BCVA) testing, standard anterior segment, and dilated fundoscopy examinations were performed followed by ophthalmic imaging.

Spectral-Domain OCT Imaging

Peripapillary RNFL thickness measurements were performed with the Spectralis OCT (Heidelberg Engineering, Heidelberg, Germany) only for screening study participants using a circular scan pattern measuring 12° in diameter. Analysis was performed with the Spectralis software version 1.10.4.0, and only patients with RNFL thickness measurements within normal limits as indicated automatically by the software were included in the study.

Further, Spectralis OCT was used to acquire macular volume scans consisting of 97 B-scans. Retinal layers were delineated using the inbuilt automated segmentation algorithm and corrected manually in each B-scan if necessary. We analyzed the mean thickness in the central ETDRS subfield, the inner (3-mm diameter, consisting of 4 parafoveal subfields) and outer (6-mm diameter, consisting of 4 perifoveal subfields) ETDRS ring for the RNFL, ganglion cell layer (GCL), and inner plexiform layer (IPL).

Swept-Source OCT Imaging

Macular volume scans were performed with the PlexElite system (Carl Zeiss Meditec, Jena, Germany) using a 6 × 6 mm scanning pattern centered on the fovea to evaluate the presence of macular edema in diabetic patients.

PS-OCT Imaging

Measurement of peripapillary RNFL birefringence was performed using a spectral-domain PS-OCT system with an integrated retinal tracker.[32] Imaging was performed with a center wavelength of 860 nm, an A-scan rate of 70 kHz, and a bandwidth of 60 nm. The resolution achieved was 4.2 µm (in tissue) axially and 20 µm laterally. For each subject, a raster scanning including the optic nerve head (ONH) and a circular scan around the ONH were acquired. The raster images consisted of 250 B-scans of 1024 A-scans each. One hundred circular B-scans of 2048 A-scans repeated at the same location around the ONH (radius: 1.5 mm; this corresponds to the center radius used for retardation imaging by SLP with the Carl Zeiss Meditec GDX-VCC instrument) were additionally acquired. After standard Fourier domain OCT processing of the data and extraction of the polarization parameters, individual corneal birefringence compensated retardation tomograms were obtained by applying an algorithm that is described in detail elsewhere and also corrected for birefringence effects introduced by other sections of the anterior eye segment including the lens.[33] Averaged intensity and retardation circumpapillary tomograms (obtained from the 50 scans best correlated to an empirically chosen single scan of high quality that is free from motion artifacts) were extracted using a method based on Stokes vector averaging[34] and used for the quantitative birefringence analysis. From the circumpapillary intensity and retardation tomograms, circumpapillary plots of RNFL birefringence were obtained by a linear fit of retardation versus depth (within the RNFL tissue) for each A-scan position. Details of the method are reported in our recent related study.[30] The reproducibility of this method has been shown to be 0.005°/µm in healthy eyes. Averaged RNFL circumpapillary birefringence is

Investigative Ophthalmology & Visual Science

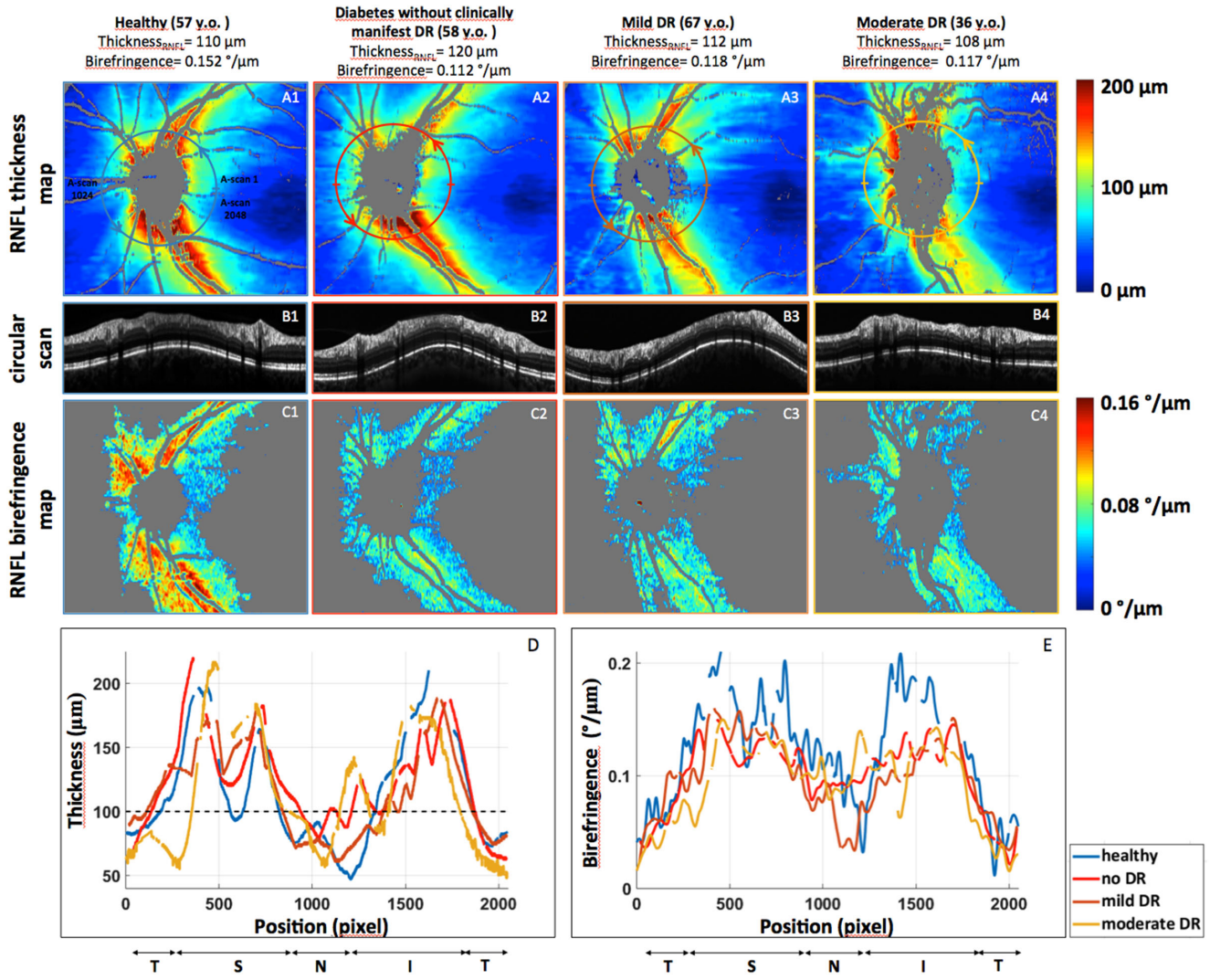

Figure 1. Representative examples of a 57-year-old healthy female eye (A1, B1, C1), a 58-year-old diabetic female eye with subclinical DR (A2, B2, C2), a 67-year-old male eye with mild DR (A3, B3, C3), and a 36-year-old male eye with moderate DR (A4, B4, C4). A1-A4: RNFL thickness (µm) maps are color coded and show the circular scan around the ONH with a radius of 1.5 mm. B1-B4: Cross-sectional intensity averaged circular scans obtained at the location indicated by the ring in A1-A4 starting from the temporal and followed by the superior quadrant. C1-C4: Birefringence (°/µm) maps are color coded and show the location of the ring from which the birefringence values are obtained. Reduced birefringence is seen in the diabetic eyes (C2-C4) compared with the healthy control subject (C1). (D, E) Graphs of peripapillary RNFL thickness (D) and birefringence (E) along the ring around the ONH are shown. Although the thickness plots appear similar among the study subjects shown, birefringence plots are higher in the healthy control subject. All values along the circumpapillary scan are shown, whereas only areas of RNFL thickness >100 µm are used for quantitative analysis, that is, areas above the dashed line in (D). I, inferior; N, nasal; S, superior; T, temporal.

calculated considering only areas of RNFL thickness >100 µm (which provide a sufficient amount of points in depth for an accurate linear fit) and after removal of the vessels (identified by the shadows they cast on the RPE). Distinction between the inferior and superior sectors is also performed. Additionally, en face RNFL thickness and birefringence maps were obtained from the raster scans. Figure 1 shows an overview of scans and maps obtained by PS-OCT imaging.

Statistical Analysis

Qualitative variables are reported as absolute frequency and percentage. For quantitative variables mean ± standard deviation are reported.

DR stages (diabetes without clinically manifest DR, mild/moderate DR, healthy controls) were compared by mixed models (SAS Proc mixed; SAS Institute Inc., Cary, NC) adjusting for age. Subject-ID was taken as random factor. If the F-test of DR stage was statistically significant, pairwise group comparisons were conducted.

To analyze the difference between superior and inferior birefringence within diabetic patients, a mixed model was calculated. The dependent variable was birefringence, the independent variable was superior (yes/no). Subject-ID and the nested effect of eye within subject were taken as random factors, whereby a compound symmetry was chosen as the covariance structure. The interaction term between DR stage and superior was also analyzed but removed from

Investigative Ophthalmology & Visual Science

the model because the *P* value of the F-test was greater than 0.05 (results not shown).

To analyze the effect of disease-related or demographic variables on birefringence (total, superior, or inferior, respectively) within diabetic patients, mixed models with subject-ID as random factor were applied. DR stage and the interaction with DR stage were included as additional independent variables. If the F-test of the interaction term revealed a *P* value >0.05, the interaction term was removed from the model. If the *P* value of DR-stage was >0.05 in the reduced model, a univariate mixed model was calculated (results of the F-tests not shown). The subgroup of healthy subjects was analyzed by paired *t*-test and univariate linear models. Mixed models were checked for influential observations. Influential observations were analyzed by diagnostic plots (restricted likelihood distance [RLD], Cook's distance, and COVRatio). An observation was excluded from the model if the following criterion was met: RLD >2 + Cook's distance >4/n + |COVRatio – 1| > 3*p/n, where n is the number of eyes and p is the number of parameters in the model (Nieuwenhuis et al. 2012[52], SAS/STAT 14.3. User's guide). Hence in the mixed models with GCL in the disc/fovea as dependent variable, one influential observation was excluded.

Because of the exploratory character of the study, no adjustment for multiple testing was done. The significance level has been set to 0.05. Statistical analyses were carried out with SAS 9.4 (SAS Institute Inc.).

Results

Seventy eyes (35 left eyes) of 43 patients (15 women) with diabetes mellitus (n = 26 type 2 and n = 17 type 1) and a mean age of 50.86 ± 15.71 years were enrolled in this prospective observational pilot study. At time of enrollment, 36 eyes had no clinically detectable DR, 17 eyes showed mild and 17 eyes moderate DR. The mean HbA1c was 7.67% ± 1.62% and mean diabetes duration 14.95 ± 9.95 years. The mean BCVA was 1.09 ± 0.15. None of the patients presented with a current DME defined by DRCR (Diabetic Retinopathy Clinical Research) Network criteria as retinal thickness in the central subfield of 250 µm or greater as assessed on cross-sectional spectral-domain OCT scans, or any previous episodes of DME as reviewed by respective medical charts and spectral-domain OCT scans.[35] One patient had uncomplicated cataract surgery in 1 eye 12 months prior to study inclusion. Table 1 summarizes the baseline characteristics of the diabetic patients. Thirty-four eyes (22 left) of 34 healthy

Table 1. Baseline Characteristics of Diabetic Patients

No. of Patients/Eyes	43/70
Sex, no. patients (%)	
Male	28 (65.12)
Female	15 (34.88)
Diabetes type, no. patients (%)	
2	26 (60.47)
1	17 (39.53)
Hb1A1C level (%), mean ± SD	7.67 ± 1.62 (2 missing)
BCVA, mean ± SD	1.09 ± 0.15
DR stage, no. eyes (%)	
No clinically detectable DR	36 (51.43)
Mild DR	17 (24.29)
Moderate DR	17 (24.29)
Insulin therapy, no. patients (%)	26 (60.47)
Diabetes duration, years, mean ± SD	14.95 ± 9.95

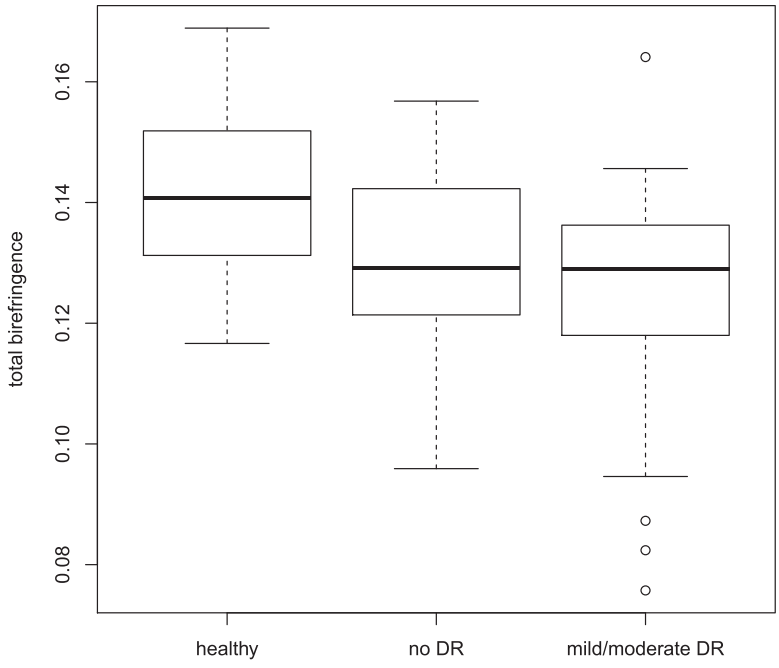

Figure 2. Comparison of total birefringence values indicated on the y-axis in ° per µm (°/µm) of peripapillary RNFL between healthy subjects and diabetics with no DR to mild/moderate DR. The comparison of healthy versus diabetes, no DR ($P = 0.0033$), and healthy versus diabetes mild/moderate DR ($P < 0.0001$) was statistically significant, whereas the difference between diabetes groups was only borderline significant (no DR vs. mild/moderate DR; $P = 0.050$). In the box plots, the inferior boundary of the box indicates the 25th percentile, a black line within the box marks the median, and the superior boundary of the box indicates the 75th percentile. Whiskers extend to the smallest/largest value within the interval [25th percentile – 1.5 x interquartile range; 75th percentile + 1.5 x interquartile range] and outliers are shown as circles. If no outliers occur, the whiskers extend to the minimum and maximum, respectively.

Investigative Ophthalmology & Visual Science

control subjects (17 women) with a mean age of 53.21 ± 13.88 years and a mean BCVA of 1.0 ± 0.1 were included.

The mean peripapillary RNFL birefringence values in eyes of diabetic patients without clinically detectable DR (n = 36) were 0.131° ± 0.014°/µm, and in eyes with mild or moderate DR (n = 34) 0.125° ± 0.018°/µm. The mean RNFL birefringence values of age-matched healthy eyes (n = 34) were 0.143° ± 0.014°/µm.

Mean total RNFL birefringence numbers were statistically significantly lower in diabetic eyes without clinically manifest DR, as well as in eyes with mild to moderate DR stages compared with healthy age-matched controls (mean difference [95% confidence interval {CI}]: –0.0124 [–0.0202; –0.0045], P = 0.0033; –0.0189 [–0.0266; –0.0111], P = < 0.0001; respectively; Fig. 2). Comparison of birefringence values between diabetic subjects with no clinically manifest DR versus mild to moderate DR stages revealed a borderline significant difference (0.0065 [–0.000004; 0.0130], P = 0.050; Fig. 2). We further subdivided the peripapillary circular scan into a superior and inferior sector. Similarly to the total birefringence results, separate analysis of either the superior or inferior half ring revealed statistically significant differences between diabetic eyes without DR and nondiabetic healthy age-matched controls (mean difference [95% CI]: –0.0127 [–0.0206; –0.0048], P = 0.0027; –0.0121 [–0.0207; –0.0036], P = 0.0069; respectively) and diabetic eyes with mild to moderate DR stages and healthy controls (–0.0174 [–0.0251; –0.0096], P < 0.0001; –0.0201 [–0.0285; –0.0117], P < 0.0001; respectively), a weak significance between diabetic eyes with no clinically manifest DR versus mild to moderate DR stages in the inferior half ring (0.0080 [0.0008; 0.0152], P = 0.0316) but no significant differences between the same groups in the superior area (0.0047 [–0.0021; 0.0115], P = 0.1668; Table 2). Across the healthy nondiabetic study subjects mean birefringence values were not significantly different between superior and inferior sectors (paired t-test: mean difference [95% CI]: –0.0038 [–0.0077; 0.00002;], P = 0.051). In contrast, diabetic eyes with no clinically detectable DR or mild to moderate DR stages showed significantly lower mean birefringence values in the inferior compared with the superior sectors (mixed model: mean difference [95% CI]: –0.0047 [–0.0068; –0.0026], P < 0.0001; Fig. 3). Diabetes duration was not statistically associated with RNFL birefringence values (total, superior, and inferior sectors). Neither sex, HbA1c, and type of diabetes categorized in type 1 or 2 showed any statistically significant associations to birefringence levels. Within the diabetes patients, a statisti-

Table 2. Peripapillary RNFL Birefringence Values Indicated in ° Per µm in Healthy and Diabetic Subjects Over all Eyes (Healthy: 34 Eyes of 34 Patients, Diabetes Without DR: 36 Eyes of 23 Patients, Mild/Moderate DR: 34 Eyes of 25 Patients)

Total Birefringence	**Mean**	**SD**	**Median**	**Q1**	**Q3**
Healthy controls	0.143	0.014	0.141	0.131	0.152
Diabetes without DR	0.131	0.014	0.130	0.121	0.142
Mild/moderate DR	0.125	0.018	0.130	0.118	0.136
Superior birefringence	**Mean**	**SD**	**Median**	**Q1**	**Q3**
Healthy controls	0.144	0.013	0.143	0.134	0.151
Diabetes without DR	0.132	0.014	0.133	0.124	0.145
Mild/moderate DR	0.128	0.018	0.130	0.121	0.139
Inferior birefringence	**Mean**	**SD**	**Median**	**Q1**	**Q3**
Healthy controls	0.140	0.016	0.140	0.131	0.150
Diabetes without DR	0.129	0.015	0.126	0.118	0.137
Mild/moderate DR	0.122	0.019	0.125	0.113	0.134

Q1, 25th percentile; Q3, 75th percentile; SD, standard deviation.

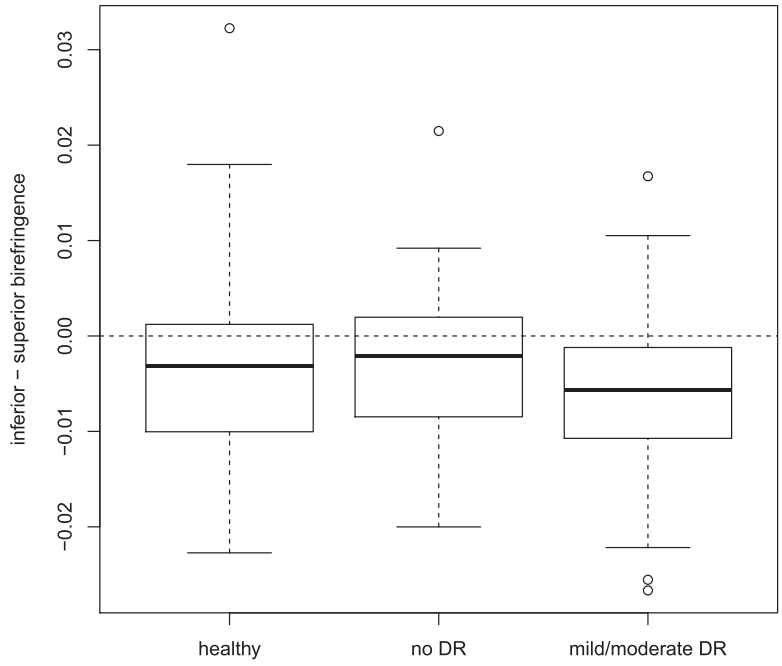

Figure 3. The mean peripapillary birefringence values indicated on the y-axis in ° per µm (°/µm) of diabetic patients are significantly lower in the inferior compared with the superior sectors (P < 0.0001) with no statistically significant difference between sectors in the healthy eyes. In the box plots, the inferior boundary of the box indicates the 25th percentile, a black line within the box marks the median, and the superior boundary of the box indicates the 75th percentile. Whiskers extend to the smallest/largest value within the interval [25th percentile – 1.5 x interquartile range; 75th percentile + 1.5 x interquartile range] and outliers are shown as circles. If no outliers occur, the whiskers extend to the minimum and maximum, respectively.

Investigative Ophthalmology & Visual Science

Table 3. Peripapillary RNFL Thickness Indicated in µm in Healthy and Diabetic Subjects; Healthy: 34 Eyes of 34 Patients, Diabetes Without DR: 36 Eyes of 23 Patients, Mild/Moderate DR: 34 Eyes of 25 Patients

Peripapillary RNFL Thickness	Mean	SD	Median	Q1	Q3
Healthy controls	114.4	12.8	115.0	108.4	124.7
Diabetes without DR	118.4	9.5	117.9	112.6	123.8
Mild/moderate DR	119.5	12.6	116.4	110.2	129.0

Q1, 25th percentile; Q3, 75th percentile; SD, standard deviation.

cally significant effect of age on birefringence total and superior could be observed in eyes with subclinical DR (total: estimate [95% CI]: –0.00042 [–0.00079; –0.00005], $P = 0.028$; superior: estimate [95% CI]: 0.00041 [–0.00079; –0.00003], $P = 0.033$), but not in eyes with mild or moderate DR (total: estimate [95% CI]: –0.00002 [–0.0004; 0.00035], $P = 0.90$; superior: estimate 0.00003 [–0.00035; 0.00041], $P = 0.86$) For birefringence inferior, the slopes did not differ significantly between the subgroups (subclinical DR, mild to moderate DR) and the effect of age was statistically not significant either (estimate [95% CI] adjusted for DR stage: –0.0026 [–0.0006; 0.00008], $P = 0.13$). Within the controls, the effect of age was statistically significant for birefringence total and superior (estimate [95% CI]: –0.0003 [–0.0007; –0.00001], $P = 0.043$; –0.0004 [–0.0007; –0.00004], $P = 0.027$, respectively) with lower birefringence values with advanced age, but not for birefringence inferior ($P = 0.0950$).

The mean peripapillary RNFL thickness in eyes with subclinical DR was 118.4 ± 9.5 µm, and in mild to moderate DR 119.5 ± 12.6 µm as assessed by PS-OCT. Healthy control eyes had a mean RNFL thickness of 114.4 ± 12.8 µm (Table 3). We could neither detect any statistically significant differences of RNFL thickness between diabetic and healthy eyes nor within diabetic eyes in our study cohort (F-test: $P = 0.46$). This analysis was performed from the data obtained with PS-OCT with all study subjects showing RNFL thickness within normal limits on Spectralis OCT measurements, which was an inclusion requirement. We further analyzed the macular ganglion cell complex (GCC) consisting of RNFL, GCL, and IPL in the foveal subfield, as well as in inner and outer rings of the ETDRS grid. Retinal thickness was automatically calculated in the nine ETDRS areas (consisting in a central circular zone with a 1-mm diameter, representing the foveal area and inner and outer rings of 3 and 6 mm diameter, respectively). When performing comparisons between our study groups, no statistically significant differences in any of the three neuroretinal layers could be observed (F-test: P values ranging from 0.062–0.78). Table 4 shows the individual neuroretinal layer thicknesses in both healthy and diabetic eyes.

Table 4. Retinal GCC Thickness of the Macular Area Indicated in µm in Healthy and Diabetic Subjects and Subdivided by ETDRS Locations (Center, Inner Ring, Outer Ring); Healthy: 34 Eyes of 34 Patients, Diabetes Without DR: 36 Eyes of 23 Patients, Mild/Moderate DR: 34 Eyes of 25 Patients

RNFL	ETDRS Location	Mean	SD	Median	Q1	Q3
Healthy controls	center	11.97	2.37	11.00	11.00	13.00
	inner	21.47	1.78	21.25	20.50	22.50
	outer	36.90	3.58	36.75	34.00	40.25
Diabetes without DR	center	12.22	2.39	12.00	11.00	14.00
	inner	21.92	1.92	22.00	20.75	23.25
	outer	37.13	3.59	37.13	34.13	40.00
Mild/moderate DR	center	13.12	2.42	13.00	11.00	15.00
	inner	22.83	2.88	22.00	21.25	24.25
	outer	38.58	4.84	38.25	34.50	40.75
GCL	**ETDRS Location**	**Mean**	**SD**	**Median**	**Q1**	**Q3**
Healthy controls	center	14.35	4.99	13.00	11.00	16.00
	inner	51.34	4.04	50.42	48.25	54.50
	outer	36.41	2.64	36.38	34.67	38.00
Diabetes without DR	center	14.75	3.44	14.50	13.00	16.50
	inner	50.67	5.08	50.63	47.75	53.63
	outer	35.99	3.48	35.38	34.38	38.75
Mild/moderate DR	center	16.55	5.93	16.00	12.00	18.00
	inner	54.08	5.35	52.75	50.75	56.50
	outer	38.08	4.05	38.25	36.00	39.75
IPL	**ETDRS Location**	**Mean**	**SD**	**Median**	**Q1**	**Q3**
Healthy controls	center	19.88	3.89	19.00	17.00	22.00
	inner	41.58	2.71	41.50	39.25	44.00
	outer	29.51	1.96	29.63	28.25	30.75
Diabetes without DR	center	20.39	3.23	20.00	18.00	23.00
	inner	42.00	3.43	42.13	40.13	44.13
	outer	29.80	2.54	29.50	28.13	31.63
Mild/moderate DR	center	22.27	4.94	22.00	19.00	24.00
	inner	43.52	3.47	42.75	41.50	44.50
	outer	31.04	2.85	31.25	29.00	32.75

Q1, 25th percentile; Q3, 75th percentile; SD, standard deviation.

Investigative Ophthalmology & Visual Science

Discussion

Diabetes is a multisystemic disease leading to neurodegenerative processes in a number of organs including the eye. In this study, we determined the polarization properties of the peripapillary region of diabetic and healthy eyes by PS-OCT to measure birefringence introduced by the RNFL. Our study revealed for the first time birefringence of the peripapillary RNFL as a novel imaging parameter significantly reduced in eyes of diabetics even without any clinically detectable signs of DR and with normal RNFL thickness. The main advantage of this technology is that both thickness and retardation data are recorded concurrently by the same device and not separately through conventional OCT and SLP. The within-subject standard deviation and repeatability measures of averaged RNFL birefringence values of the PS-OCT device used in our study has recently been investigated in human eyes by Desissaire et al.[30] and showed excellent repeatability measurements (precision of 0.005°/µm).

There is solid evidence of the critical role of neuroretinal degenerative processes in the pathogenesis of DR by ex vivo analyses showing the involvement of retinal ganglion cell bodies and dendrites, which are visualizable by in vivo OCT imaging through thinning of GCL and IPL.[36] Consequently, associated axons may become apoptotic with thinning of the RNFL.[37] However, results regarding thickness measurements of specific inner retinal layers in the macular region of diabetic eyes with different DR stages are inconsistent throughout the literature. There are studies showing evidence of GCL and IPL thinning in diabetics[38,39] even in the absence of any DR,[2,38,40] whereas Verma et al.[41] report thicker GCL layers in diabetic subjects compared with healthy controls. Loss of RNFL in diabetic eyes with no to minimal DR compared with controls was shown,[2,42] with other studies demonstrating no differences in diabetic eyes.[41,43] Macular thickness in diabetic patients varies greatly with disease progression already in subclinical stages and even more when macular edema develops. Therefore macular evaluation in diabetic eyes should be performed with caution as hyperglycemia might activate intraretinal immune-mediated pathways leading to inflammation with swelling of specific layers and masking of neurodegenerative changes.[1] We meticulously analyzed OCT scans of subjects for the presence of macular edema before inclusion in our study, and additionally studied all available medical records to rule out any previous fluid accumulation. Analyses of the macular GCC in our study cohort revealed no significant differences between healthy controls and diabetic subjects with or without early DR stages in any of the retinal GCC layers. The RNFL, GCL, and IPL findings for diabetic eyes without DR and control groups are in line with Vujosevic et al.,[44] yet they found significant reductions in some parts of the outer ETDRS ring of diabetics without DR compared with eyes with nonproliferative DR. As the peripapillary RNFL layer contains a considerably higher density of axons compared with the macular region, it may constitute a more appropriate location to evaluate neurodegenerative processes. To date morphologic evaluation consists of RNFL thickness measurements and reductions in the average RNFL thickness of diabetic patients even without DR were reported by several studies.[41,45,46] In contrast, studies by Ng et al.[40] and Vujosevic et al.[44] showed that peripapillary RNFL thickness was not significantly different between diabetic eyes and healthy controls, including subjects without signs of DR after age correction. Overall data currently available point to an early involvement of neurodegeneration in the pathogenesis of DR with no distinct parameters yet elucidated by conventional OCT imaging.

Previous studies showed that RNFL birefringence varies across the entire ONH area in healthy subjects.[20,23,27] In diabetic patients, mean birefringence values are lower in the inferior compared with the superior sectors across our study cohort independent of diabetes stage. The exact reason why there is a regional variation of RNFL birefringence in diabetic eyes is not known but may be due to thinner sizes of axons in the inferior sectors, which are potentially more vulnerable to degeneration under hyperglycemic conditions. Another hypothesis is that minuscule intraretinal fluid accumulation preferably in inferior sectors that are not visualizable with current state-of-the-art imaging modalities may cause a reduction of birefringence values. Interestingly, also in glaucoma an increased vulnerability of inferior as opposed to superior RNFL has been described.[47] Interestingly, we could only detect borderline significant differences of birefringence levels between diabetics without DR and with mild/moderate DR. This finding may be related to a potential ceiling effect of the birefringence signal or caused by other parameters, such as duration or levels of hyperglycemia.

Detailed manual RNFL thickness measurements on scans obtained by PS-OCT resulted in no statistically significant thickness changes among our study population, which was selected by normal RNFL thickness measurements by Spectralis OCT, implying that the observed reduced birefringence values are independent of it. Based on findings from glaucomatous neuropathy studies in a nonhuman primate model, ganglion cell axon density may be altered before a reduction of RNFL thickness[48,49] with comparable timely sequences potentially occurring during the pathogenesis of DR.

We could not find any correlation between birefringence reduction and diabetes duration, which ranged from less than 1 year to 35 years in our study cohort. The exact time of diabetes onset is often unknown as it may precede the clinical diagnosis by years. Reductions in RNFL birefringence were comparable in type 1 and 2 diabetic patients based on our mixed model calculations, which may not be obvious due to pathophysiological differences between the two diabetes types with type 1 diabetics presenting with lower plasma insulin concentrations.[50]

Our study has several limitations. First, we did not measure ocular axial length, which may influence RNFL measurements.[51] However, the refractive error of our patients was within a narrow range between +2 and –3 diopters and no patient underwent refractive surgery. It cannot be excluded that some of the controls also had type 2 diabetes as the disease may have a subclinical course and HbA1c levels were unknown. However, the existence of undiagnosed diabetes would most likely lead to underestimation of the difference of birefringence values between patients and controls.

The capability of PS-OCT to provide precise quantitative data on peripapillary RNFL birefringence might serve as an early indicator of RDN. However, further studies are needed and currently planned at our site based on this pilot study with larger patient numbers to investigate in particular the effect of diabetes duration, HbA1c levels, and more advanced DR stages on birefringence levels. Additionally, correlations between retinal sensitivity

measured by fundus-controlled microperimetry and birefringence values are needed to study the relationship between structural and functional deficits in preclinical DR eyes. If the findings from our study can be confirmed, birefringence measurements may enable early detection of RDN beyond the possibility of current state-of the art imaging technologies.

Conclusions

This study provides a first description of peripapillary RNFL birefringence as a novel imaging parameter significantly reduced already in subclinical DR compared with healthy controls. These results support the concept that diabetes causes primary alterations to neuroretinal tissues before microvascular damage occurs.

Acknowledgments

Supported by the Austrian Science Fund (FWF Grant number: P30378).

Disclosure: **A. Pollreisz**, None; **S. Desissaire**, None; **A. Sedova**, None; **D. Hajdu**, None; **F. Datlinger**, None; **F. Schwarzhans**, None; **S. Steiner**, None; **I. Steiner**, None; **C. Vass**, None; **C.K. Hitzenberger**, None; **M. Pircher**, None; **U. Schmidt-Erfurth**, None

References

1. Antonetti DA, Klein R, Gardner TW. Diabetic retinopathy. *N Engl J Med.* 2012;366:1227–1239.
2. Sohn EH, van Dijk HW, Jiao C, et al. Retinal neurodegeneration may precede microvascular changes characteristic of diabetic retinopathy in diabetes mellitus. *Proc Natl Acad Sci.* 2016;113:E2655–E2664.
3. Drasdo N, Chiti Z, Owens DR, et al. Effect of darkness on inner retinal hypoxia in diabetes. *Lancet.* 2002;359:2251–2253.
4. Gualtieri M, Bandeira M, Hamer RD, et al. Contrast sensitivity mediated by inferred magno- and parvocellular pathways in type 2 diabetics with and without nonproliferative retinopathy. *Invest Ophthalmol Vis Sci.* 2011;52:1151–1155.
5. Han Y, Adams AJ, Bearse MA, Jr, et al. Multifocal electroretinogram and short-wavelength automated perimetry measures in diabetic eyes with little or no retinopathy. *Arch Ophthalmol.* 2004;122:1809–1815.
6. Realini T, Lai MQ, Barber L. Impact of diabetes on glaucoma screening using frequency-doubling perimetry. *Ophthalmology.* 2004;111:2133–2136.
7. Falsini B, Porciatti V, Scalia G, et al. Steady-state pattern electroretinogram in insulin-dependent diabetics with no or minimal retinopathy. *Doc Ophthalmol Advances Ophthalmol.* 1989;73:193–200.
8. Fujimoto JG, Drexler W, Schuman JS, et al. Optical coherence tomography (OCT) in ophthalmology: introduction. *Opt Express.* 2009;17:3978–3979.
9. Bussel II, Wollstein G, Schuman JS. OCT for glaucoma diagnosis, screening and detection of glaucoma progression. *Br J Ophthalmol.* 2014;98(suppl 2):ii15–ii19.
10. Petzold A, de Boer JF, Schippling S, et al. Optical coherence tomography in multiple sclerosis: a systematic review and meta-analysis. *Lancet Neurol.* 2010;9:921–932.
11. Yu JG, Feng YF, Xiang Y, et al. Retinal nerve fiber layer thickness changes in Parkinson disease: a meta-analysis. *PLoS One.* 2014;9:e85718.
12. Thomson KL, Yeo JM, Waddell B, et al. A systematic review and meta-analysis of retinal nerve fiber layer change in dementia, using optical coherence tomography. *Alzheimer Dementia.* 2015;1:136–143.
13. Hee DH MR, Swanson EA, Fujimoto JG. Polarization-sensitive low-coherence reflectometer for birefringence characterization and ranging. *J Opt Soc Am.* 1992;9:903–908.
14. Dave DP, Akkin T, Milner TE. Polarization-maintaining fiber-based optical low-coherence reflectometer for characterization and ranging of birefringence. *Opt Letters.* 2003;28:1775–1777.
15. de Boer JF, Milner TE, van Gemert MJ, et al. Two-dimensional birefringence imaging in biological tissue by polarization-sensitive optical coherence tomography. *Opt Letters.* 1997;22:934–936.
16. Cense B, Chen TC, Park BH, et al. In vivo depth-resolved birefringence measurements of the human retinal nerve fiber layer by polarization-sensitive optical coherence tomography. *Opt Letters.* 2002;27:1610–1612.
17. Hitzenberger C, Goetzinger E, Sticker M, et al. Measurement and imaging of birefringence and optic axis orientation by phase resolved polarization sensitive optical coherence tomography. *Opt Express.* 2001;9:780–790.
18. Pircher M, Hitzenberger CK, Schmidt-Erfurth U. Polarization sensitive optical coherence tomography in the human eye. *Prog Retin Eye Res.* 2011;30:431–451.
19. Lopes de Faria JM, Russ H, Costa VP. Retinal nerve fibre layer loss in patients with type 1 diabetes mellitus without retinopathy. *Br J Ophthalmol.* 2002;86:725–728.
20. Mujat M, Park BH, Cense B, et al. Autocalibration of spectral-domain optical coherence tomography spectrometers for in vivo quantitative retinal nerve fiber layer birefringence determination. *J Biomed Opt.* 2007;12:041205.
21. Gotzinger E, Pircher M, Baumann B, Hirn C, Vass C, Hitzenberger CK. Retinal nerve fiber layer birefringence evaluated with polarization sensitive spectral domain OCT and scanning laser polarimetry: a comparison. *J Biophotonics.* 2008;1:129–139.
22. Yamanari M, Miura M, Makita S, et al. Phase retardation measurement of retinal nerve fiber layer by polarization-sensitive spectral-domain optical coherence tomography and scanning laser polarimetry. *J Biomed Opt.* 2008;13:014013.
23. Zotter S, Pircher M, Gotzinger E, et al. Measuring retinal nerve fiber layer birefringence, retardation, and thickness using wide-field, high-speed polarization sensitive spectral domain OCT. *Invest Ophthalmol Vis Sci.* 2013;54:72–84.
24. Pircher M, Gotzinger E, Leitgeb R, et al. Imaging of polarization properties of human retina in vivo with phase resolved transversal PS-OCT. *Opt Express.* 2004;12:5940–5951.
25. Pircher M, Gotzinger E, Findl O, et al. Human macula investigated in vivo with polarization-sensitive optical coherence tomography. *Invest Ophthalmol Vis Sci.* 2006;47:5487–5494.
26. Weinreb RN, Dreher AW, Coleman A, et al. Histopathologic validation of Fourier-ellipsometry measurements of retinal nerve fiber layer thickness. *Arch Ophthalmol.* 1990;108:557–560.
27. Cense B, Chen TC, Park BH, et al. Thickness and birefringence of healthy retinal nerve fiber layer tissue measured with polarization-sensitive optical coherence tomography. *Invest Ophthalmol Vis Sci.* 2004;45:2606–2612.
28. Brink HB, van Blokland GJ. Birefringence of the human foveal area assessed in vivo with Mueller-matrix ellipsometry. *J Opt Soc Am, Opt Image Sci.* 1988;5:49–57.
29. Cense B, Wang Q, Lee S, et al. Henle fiber layer phase retardation measured with polarization-sensitive optical

coherence tomography. *Biomed Opt Express.* 2013;4:2296–2306.

30. Desissaire S, Pollreisz A, Sedova A, et al. Analysis of retinal nerve fiber layer birefringence in patients with glaucoma and diabetic retinopathy by polarization sensitive OCT. *Biomed Opt Express.* 2020;11:5488–5505.
31. Grading diabetic retinopathy from stereoscopic color fundus photographs–an extension of the modified Airlie House classification. ETDRS report number 10. Early Treatment Diabetic Retinopathy Study Research Group. *Ophthalmology.* 1991;98(5 suppl):786–806.
32. Sugita M, Zotter S, Pircher M, et al. Motion artifact and speckle noise reduction in polarization sensitive optical coherence tomography by retinal tracking. *Biomed Opt Express.* 2013;5:106–122.
33. Pircher M, Gotzinger E, Baumann B, et al. Corneal birefringence compensation for polarization sensitive optical coherence tomography of the human retina. *J Biomed Opt.* 2007;12:041210.
34. Sugita M, Pircher M, Zotter S, et al. Retinal nerve fiber bundle tracing and analysis in human eye by polarization sensitive OCT. *Biomed Opt Express.* 2015;6:1030–1054.
35. Diabetic Retinopathy Clinical Research Network;Beck RW, Edwards AR, et al. Three-year follow-up of a randomized trial comparing focal/grid photocoagulation and intravitreal triamcinolone for diabetic macular edema. *Arch Ophthalmol.* 2009;127:245–251.
36. Simo R, Stitt AW, Gardner TW. Neurodegeneration in diabetic retinopathy: does it really matter? *Diabetologia.* 2018;61:1902–1912.
37. Barber AJ. A new view of diabetic retinopathy: a neurodegenerative disease of the eye. *Prog Neuropsychopharmacol Biol Psychiatry.* 2003;27:283–290.
38. Chhablani J, Sharma A, Goud A, et al. Neurodegeneration in type 2 diabetes: evidence from spectral-domain optical coherence tomography. *Invest Ophthalmol Vis Sci.* 2015;56:6333–6338.
39. Gundogan FC, Akay F, Uzun S, et al. Early neurodegeneration of the inner retinal layers in type 1 diabetes mellitus. *Ophthalmol J.* 2016;235:125–132.
40. Ng DS, Chiang PP, Tan G, et al. Retinal ganglion cell neuronal damage in diabetes and diabetic retinopathy. *Clin Exp Ophthalmol.* 2016;44:243–250.
41. Verma A, Raman R, Vaitheeswaran K, et al. Does neuronal damage precede vascular damage in subjects with type 2 diabetes mellitus and having no clinical diabetic retinopathy? *Ophthalmic Res.* 2012;47:202–207.
42. Garcia-Martin E, Cipres M, Melchor I, et al. Neurodegeneration in patients with type 2 diabetes mellitus without diabetic retinopathy. *J Ophthalmol.* 2019;2019:1825819.
43. Scarinci F, Picconi F, Virgili G, et al. Single retinal layer evaluation in patients with type 1 diabetes with no or early signs of diabetic retinopathy: the first hint of neurovascular crosstalk damage between neurons and capillaries? *Ophthalmol J.* 2017;237:223–231.
44. Vujosevic S, Midena E. Retinal layers changes in human preclinical and early clinical diabetic retinopathy support early retinal neuronal and Muller cells alterations. *J Diab Res.* 2013;2013:905058.
45. Salvi L, Plateroti P, Balducci S, et al. Abnormalities of retinal ganglion cell complex at optical coherence tomography in patients with type 2 diabetes: a sign of diabetic polyneuropathy, not retinopathy. *J Diab Compl.* 2016;30:469–476.
46. Chen Y, Li J, Yan Y, Shen X. Diabetic macular morphology changes may occur in the early stage of diabetes. *BMC Ophthalmol.* 2016;16:12.
47. Hood DC, Raza AS, de Moraes CG, et al. Glaucomatous damage of the macula. *Prog Ret Eye Res.* 2013;32:1–21.
48. Weber AJ, Kaufman PL, Hubbard WC. Morphology of single ganglion cells in the glaucomatous primate retina. *Invest Ophthalmol Vis Sci.* 1998;39:2304–2320.
49. Fortune B, Burgoyne CF, Cull G, et al. Onset and progression of peripapillary retinal nerve fiber layer (RNFL) retardance changes occur earlier than RNFL thickness changes in experimental glaucoma. *Invest Ophthalmol Vis Sci.* 2013;54:5653–5661.
50. Reiter CE, Gardner TW. Functions of insulin and insulin receptor signaling in retina: possible implications for diabetic retinopathy. *Prog Ret Eye Res.* 2003;22:545–562.
51. Ueda K, Kanamori A, Akashi A, et al. Effects of axial length and age on circumpapillary retinal nerve fiber layer and inner macular parameters measured by 3 types of SD-OCT instruments. *J Glaucoma.* 2016;25:383–389.
52. Nieuwenhuis R, Pelzer B, te Grotenhuis M. influence.ME: Tools for detecting influential data inmixed effects models, 2012, http://CRAN.Rproject.org/package=influence.ME.

Investigative Ophthalmology & Visual Science